Statistical studies on the sputtering responses preparing for the MAVEN mission

Yung-Ching Wang[1]
Janet G. Luhmann[1], Francois Leblanc[2], Xiaohua Fang[3], Ronan Modolo[2], Robert Lillis[1], Justin Deighan[3], Robert E. Johnson[4], Yingjuan Ma[5], and Wing-Huen Ip[6]
1. Space Sciences Laboratory, University of California at Berkeley, USA. **2.** LATMOS/IPSL-CNRS, Université Pierre et Marie Curie, France. **3.** Laboratory for Atmospheric and Space Physics, University of Colorado, USA. **4.** Department of Engineering Physics, University of Virginia, USA. **5.** Institute of Geophysics and Planetary Physics, University of California at Los Angeles, USA. **6.** Institute of Astronomy and Space Science, National Central University, Taiwan, ROC. **E-mail address:** jinnee.ycwang@ssl.berkeley.edu (Yung-Ching Wang)

45th Annual Meeting
Division for Planetary Sciences
Denver, Colorado | 6-11 October 2013

Abstract

Since the MAVEN mission will obtain information on the pick-up ion densities and speeds, atmospheric neutrals and ions, and UV emission profiles, the atmospheric sputtering by the re-impact of the heavy pick-up ions incident on Mars can be evaluated and compared with photo-induced loss processes under a variety of solar conditions occurring during the mission. Based on the simulation results from a 3D Monte Carlo model coupled to a molecular dynamic calculation, the atmospheric sputtering efficiencies due to pick-up O^+ for a number of energy and angle spectra are studied statistically. The sputtered hot neutrals populating the extended corona and the escape components are estimated when various solar wind conditions and solar cycle variations are considered. We find that the sputtering efficiencies can be characterized by the total incident fluxes as weighted with different incident energies. The dependencies between the incident pick-up ions and the sputtered hot neutrals lead to certain "response relations". These can be utilized to predict the sputtering rate when incident pick-up O^+ fluxes become available. A sputtered hot neutral corona can then be constructed as a reference before modeling results are generated.

1. Introduction

- The re-impact of the pick-up O^+ could have played a role in earlier epochs and at solar maximum in the present epoch [J.G. Luhmann et al., *GRL 19, 2151-2154*, 1992].
- The night-side sputtering can contribute hot corona at anti-sunward hemisphere [L. Li et al., *JGR 116, A08204*, 2011].

2.1 Pick-up O^+ precipitation simulation results

- The electromagnetic fields from six different cases are simulated with MHD model [Y. Ma et al., *JGR 109, A07211*, 2004; Y. Ma and A. F. Nagy, *GRL 34, L08201*, 2007]. The resultant pick-up O+ precipitations are calculated with Monte Carlo method based on the MHD results [X. Fang et al., *JGR 113, A02210*, 2008; X. Fang et al., *GRL 20, 1-6*, 2013]. See Table 1 and Table 2.
- Note that only specific IMF orientation is studied for the present time.

Table 1. Parameters of the six simulated cases.

Cases	n_{sw}	V_{sw}	IMF	Crustal field	Solar cycle
Quiet	4 cm^{-3}	400 km/s	3 nT Parker spiral toward Mars	noon	Maximum
Active	4 cm^{-3}	1200 km/s	3 nT ($+B_y$)	noon	Maximum
Extreme	20 cm^{-3}	1000 km/s	20 nT ($+B_y$)	noon	Maximum
noonC	4 cm^{-3}	400 km/s	3 nT Parker spiral toward Mars	noon	Minimum
dawnC	4 cm^{-3}	400 km/s	3 nT Parker spiral toward Mars	dawn	Minimum
NoC	4 cm^{-3}	400 km/s	3 nT Parker spiral toward Mars	Not included	Minimum

Table 2. Simulated pick-up O^+ precipitation rates.

Cases	Precipitation rate	Avg. energy flux	Avg. incident angle
Quiet	1×10^{25} s^{-1}	4×10^{8} eV cm^{-2} s^{-1}	47 deg
Active	3×10^{25} s^{-1}	1×10^{9} eV cm^{-2} s^{-1}	50 deg
Extreme	9×10^{25} s^{-1}	3×10^{10} eV cm^{-2} s^{-1}	50 deg
noonC	6×10^{24} s^{-1}	7×10^{7} eV cm^{-2} s^{-1}	48 deg
dawnC	7×10^{24} s^{-1}	1×10^{8} eV cm^{-2} s^{-1}	46 deg
NoC	4×10^{24} s^{-1}	9×10^{7} eV cm^{-2} s^{-1}	53 deg

∗EUV (1026-15Å) at Mars = 5 $\times10^{11}$ eV cm^{-2} s^{-1}

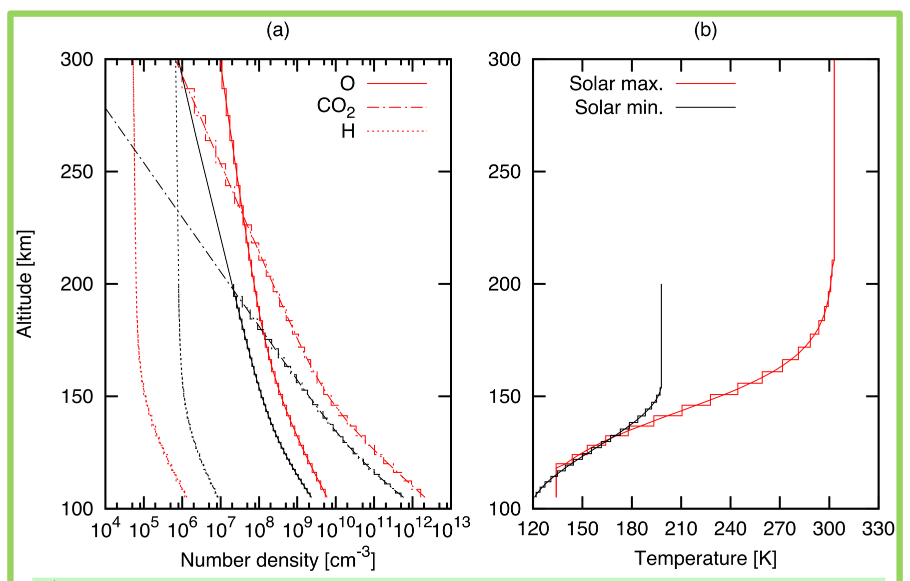

Figure 1. Uniform background atmospheric number densities and temperature distributions (Ma et al., 2004) used in the sputtering model.

2.2 Atmospheric sputtering simulation

- A Monte Carlo model of the upper atmosphere coupled to a molecular dynamic calculation [F. Leblanc and R. E. Johnson, *JGR 107, 5010*, 2002] is used to simulate the pick-up O^+ sputtering.
- The background atmospheres are shown in Figure 1 [Y. Ma et al., *JGR 109, A07211*, 2004].

3. Sputtering responses to pick-up O^+ precipitations

- The pick-up O^+ precipitation flux and the resultant sputtered hot coronae and the escape rates of O and CO_2 distributions for the quiet case are shown in Figure 2.
- The sputtering response relations respect to the incident O^+ fluxes are shown in Figure 3.

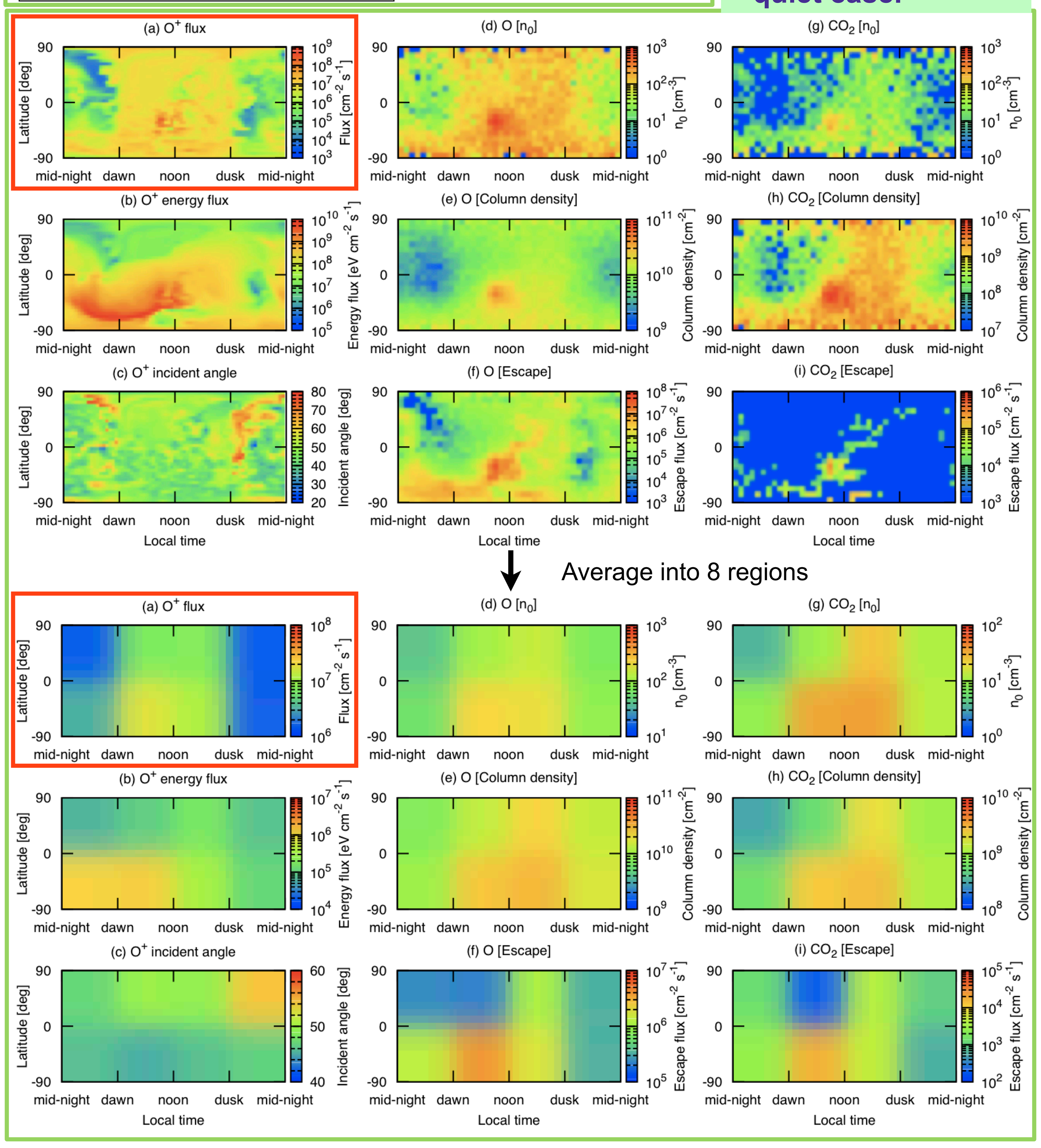

Figure 2. The pick-up O^+ precipitation distributions and the resultant sputtered hot coronae and the escape rates of O and CO_2 for the quiet case.

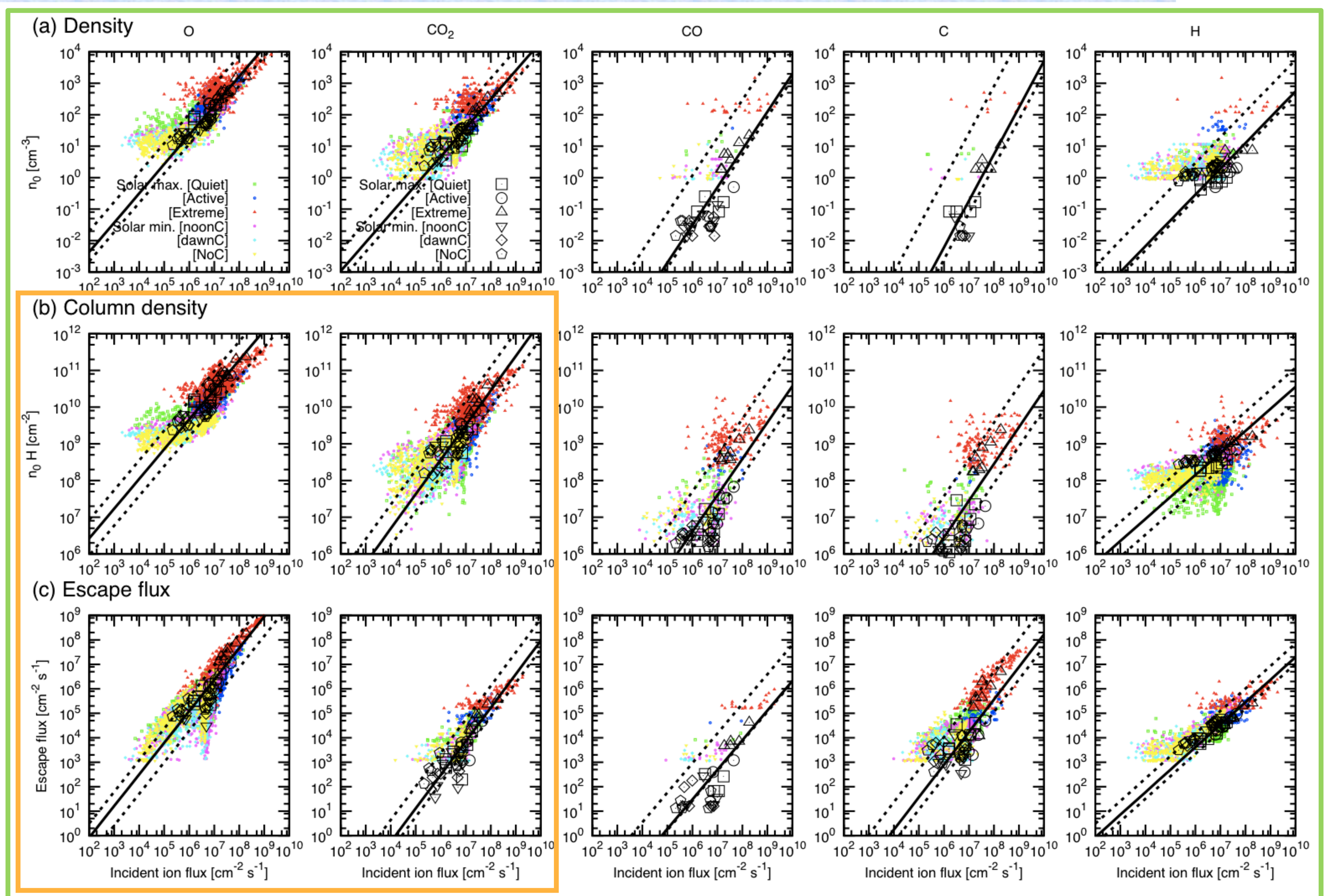

Figure 3. Sputtering responses including reference densities [n_0] (right above the exobase ~ 200-300 km) and column densities of the hot coronae, and the escape rates for different neutral species respect to the incident pick-up O+ fluxes for six simulated cases. Colored labels are the original simulated results, and the black labels are the averaged ones (see Figure 2.).

Table 3. Fitting parameters and the standard deviations.

Fit value	Fit slope	O	CO2	CO	C	H
Reference density	S	0.93	0.91	1.20	1.48	0.82
	C	2.09	2.67	6.26	7.44	3.34
	+ε	0.66	0.66	1.58	2.16	1.00
	-ε	0.30	0.30	0.16	0.38	0.13
Column density	S	0.81	0.94	0.99	1.00	0.60
	C	-6.87	-3.37	-0.72	-0.45	-10.25
	+ε	0.51	0.65	1.09	1.12	0.52
	-ε	0.46	0.46	0.46	0.52	0.43
Escape rate	S	1.29	1.37	1.21	1.33	0.92
	C	2.96	5.26	5.47	4.81	1.72
	+ε	0.58	0.90	1.48	1.13	0.56
	-ε	0.80	0.35	0.05	0.51	0.27

- **Response relation fitting**

Under the limitation of simulated number of super-particles, the "response relations" are fitted with the averaged values (black labels in Figure 3) to minimize the statistical problem for the minor species. Still, the standard deviations (ε) are calculated with the original ones (colored labels in Figure 3). The fitting and deviation equations are as follows, (see Table 3)

$$\log\left(f_{fit}\right) = S\left[\log\left(f_{ion}\right) - C\right]$$

$$\bar{\varepsilon} = \sqrt{\frac{\sum_{i=0}^{n}\left[\log\left(f_{sim}\right) - \log\left(f_{fit}\right)\right]^2}{n}}$$

f_{ion}: O^+ flux
f_{fit}: fitted values
f_{sim}: original simulated values [in MKS units]

- **Incident pick-up O^+ spectrum groups**

Since the change of the structure of the simulated upper atmosphere (Figure 1) has negligible effects on altering the sputtering responses (Y.-C. Wang et al., *JGR*, *under review*), the differences in the incident ion spectrum take charge of the scattering of the response relations. Therefore, we catalogue three different energy spectrum groups respect to the calculated standard deviations listed in Table 3. The averaged spectra and the fitting slopes are shown in Figure 4. The spectrum slopes are fitted as

$$\log\left(df_e\right) = C_s - S_s \log\left(E\right)$$

df_e: spectrum flux [cm^{-2} s^{-1} eV^{-1}]
E: energy [eV]

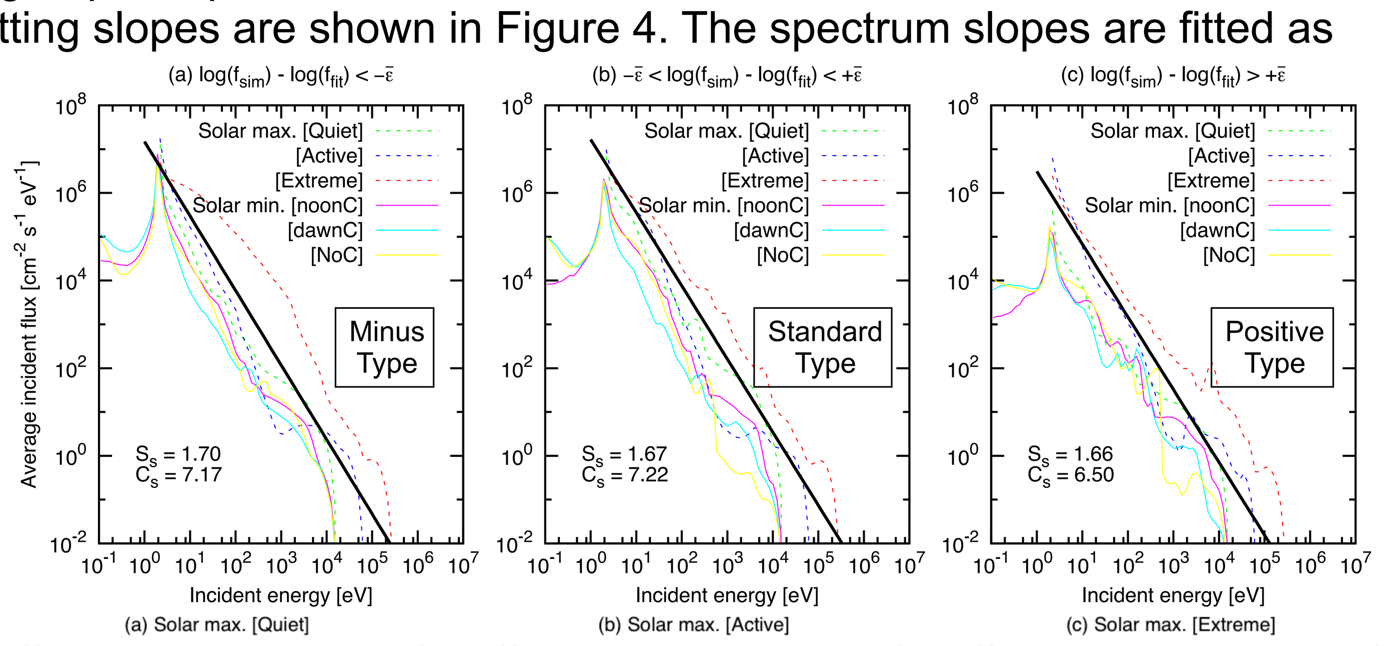

Figure 4. Averaged spectra of three catalog groups, which are separated by the standard deviations in Table 3. (Only the column densities and the escape rates of O and CO_2 are taken into considerations.)

- The "minus type" spectra have larger portion of ions with lower energies, whereas the "positive type" ones have more ions with higher energies respect to the "standard type".

We further fit all the incident pick-up O^+ spectra and catalogue them in to three labels as

-1) S_s > 1.70
0) 1.70 > S_s > 1.66
1) S_s < 1.66

Figure 5 shows the spectrum catalog distributions and Figure 6 shows the incident ion flux distributions for comparisons.

- With stronger crustal fields, the incident ion spectrum will be modulated into "minus type" one, resulting to lower sputtering efficiencies.

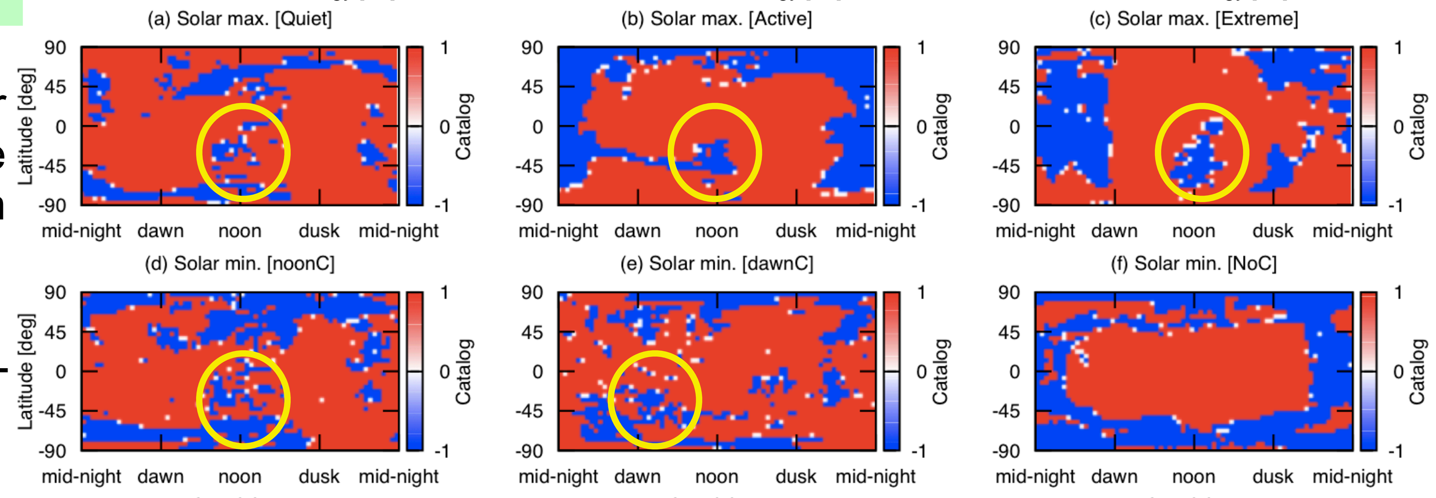

Figure 5. Incident ion spectrum catalog distributions.

Figure 6. Incident ion flux distributions for six simulated cases.